GSJ: Volume 10, Issue 6, June 2022, Online: ISSN 2320-9186

www.globalscientificjournal.com

Dynamic Modeling of a Rotor Cage Permanent Magnet Synchronous Generator with Capacitor Assistance

Emmanuel Chinweikpe Obuah[1], Otonye Ene Ojuka[2], Enyinda Igochukwu Wodi[3], Ikonwa Wonodi[4]

1-4 Department of Electrical Engineering, Faculty of Engineering, Rivers State University, Port Harcourt, Nigeria,

Corresponding author: emmanuel.obuah@ust.edu.ng.

Abstract

In this paper, a dynamic characteristic of a caged rotor permanent magnet synchronous generator (IPMSG) with capacitive assistance was studied. A balance three-phase capacitor is connected across the generator terminal loads to aid in self-excitation. A detailed mathematical modeling of the self-excited IPMSG system is presented. The proposed analysis is based on the Park's qd0-axis model of the IPMSG. Magnetic saturation is taken into account and is assumed to be confined to both the direct and quadrature axis making the dq inductances; and depends on the value of the magnetizing current. Effect of variation on the generated output voltage and electromagnetic torque are presented and discussed. The presented results show the effectiveness of capacitor on the IPMSG. This system proposed feasibility and validity are simulated on MATLAB/Simulink. The study was performed for a four-pole, three-phase, 1.250 kVA, 110 V, 1500 rpm IPMSG.

Keywords: Capacitor, dynamic modeling, rotor cage IPMSG, voltage build-up, electromagnetic torque

1. Introduction

The interest in the use of self-excited PMSGs is well known. This is as results of the shortcomings of other self-excited generators, which include dependence of the output frequency and voltage on load and prime mover speed (for self-exited induction generator) and poor power factor as well as low output power (for self-excited synchronous reluctance generator) [1-11]. Research work on PMSGs have been reported in [12-30]. Most of the studies discussed the steady-state performance and characteristics analysis of IPMSGs [12-22]. In

[23, 24], the authors worked on permanent magnet assisting a normal synchronous generator in order to reduce the magnetic saturation in the rotor-pole bodies and direct flux linkage of the armature windings from the permanent magnet. The study revealed that the efficiency of the IPMSG was better than that of the normal synchronous generator. It is fundamental that more losses will be incurred in the regular synchronous generator due to field winding of the machine. In [25-27]. the authors developed a mathematical model of single rotor single stator configuration of axial flux permanent magnet synchronous machine. Results obtained are commendable; but this was for an exterior-rotor, which is characterized with low inductance. Researchers who worked on dynamic characteristic of permanent magnet assisted synchronous reluctance generator for improve voltage build-up are found in [28].

The work in [29] did a dynamic analysis of a typical configuration of a wind turbine system equipped with a variable speed PMSG with salient rotor. A good curve for power-speed characteristics was obtained for the generator, but the dq-axis magnetic saturation was not considered. Similar works were done in [30-31], where a mathematical model of a PMSG was developed and simulated for wind energy application These were reported for an IPMSG without rotor conductors. Commendable results were also obtained but core loss and the dq-axis magnetic saturation were not considered as well.

In [32], the authors carried out modelling of transients in an IPMSG using the natural abc frame of reference. The study considered the generator with multiple damping circuits; and results obtained are commendable. However, it is realized that using the natural abc reference of frame is cumbersome when it comes to inductance calculation, which is dependent on the rotor position.

Despite many attractive features of the IPMSG in terms of reliability and robustness, the self-excited PMSG with rotor conductors has found limited report involving a scheme where the d-q inductances are accounted for as well as the core loss resistance. The one reported in [32] did not consider the transient as a result of capacitor variation, and the d-q magnetic inductances saturation was not considered as well. In fact, transient characteristics of IPMSGs should be studied under these conditions.

2. Mathematical model of the generator, capacitor and load

The conceptual winding schematic and connection diagram representing the IPMSG with rotor (damper) conductors is illustrated in Figure 1. The connection diagram is used to describe the dynamic mathematical model of the IPMSG. The analysis that follows uses the rotor reference-frame model for the analysis. The d-q rotor reference-frame voltage equations for an IPMSG can be written directly from the equations of a salient-pole synchronous generator [29-31] but with field winding terms omitted. In this paper the following simplifying assumptions have been made: One, both the d-axis and q-axis magnetizing inductances are affected

by magnetic saturation to ensure more accuracy. Two, core loss is included and is calculated by finite element procedure from a companion paper [32]. Third, there is negligible space harmonics in the air-gap flux and time harmonics in the electromotive force and current waveforms. The stator and rotor voltage equations in synchronous rotating frame are expressed as equations (1) through (4)

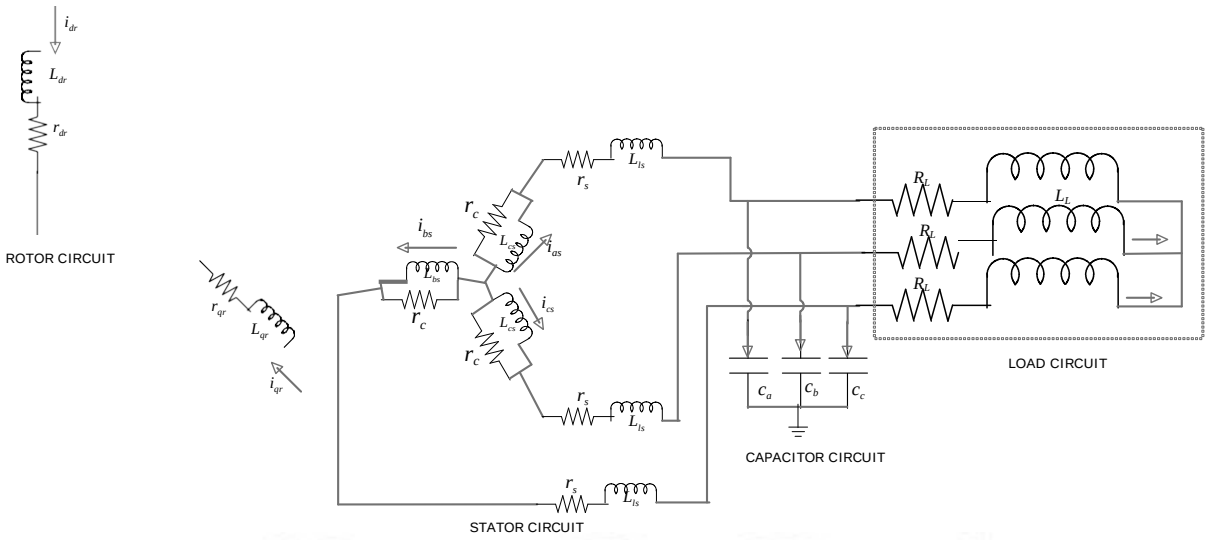

Figure 1 Conceptual winding schematic and connection diagram of the three-phase caged rotor IPMSG.

:

$$v_{qs} = p\lambda_{qs} + \omega_e\lambda_{ds} - i_{qs}r_s \tag{1}$$

$$v_{ds} = p\lambda_{ds} - \omega_e\lambda_{qs} - i_{ds}r_s \tag{2}$$

$$v'_{qr} = p\lambda'_{qr} + i'_{qr}r'_{qr} \tag{3}$$

$$v'_{dr} = p\lambda'_{dr} + i'_{dr}r'_{dr} \tag{4}$$

where the operator $p = \frac{d}{dt}$.

Equations (1) through (4) are modified and merged as (5).

$$\begin{bmatrix} v_{qs} \\ v_{ds} \\ v'_{qs} \\ v'_{ds} \end{bmatrix} = \begin{bmatrix} -r_s & 0 & 0 & 0 \\ 0 & -r_s & 0 & 0 \\ 0 & 0 & r'_{qr} & 0 \\ 0 & 0 & 0 & r'_{dr} \end{bmatrix} \begin{bmatrix} i_{qs} \\ i_{ds} \\ i'_{qr} \\ i'_{dr} \end{bmatrix} + p \begin{bmatrix} \lambda_{qs} \\ \lambda_{ds} \\ \lambda'_{qr} \\ \lambda'_{dr} \end{bmatrix} + \begin{bmatrix} 0 & \omega_e & 0 & 0 \\ -\omega_e & 0 & 0 & 0 \\ 0 & 0 & 0 & 0 \\ 0 & 0 & 0 & 0 \end{bmatrix} \begin{bmatrix} \lambda_{qs} \\ \lambda_{ds} \\ \lambda'_{qr} \\ \lambda'_{dr} \end{bmatrix} \tag{5}$$

The S subscript denotes variables and parameters associated with the stator circuits, and the r subscript denotes variables and parameters associated with the rotor circuits. The primed quantities are rotor quantities referred to the stator side.

The stator and rotor winding flux linkages of the generator with rotor cage can be expressed as (6) through (9).

$$\lambda_{qs} = -\left(L_{ls} + L_{mq}\right)i_{qs} - L_{mq}i'_{qr} = -L_{qs}i_{qs} - L_{mq}i'_{qr} \quad (6)$$

$$\lambda_{ds} = -\left(L_{ls} + L_{md}\right)i_{ds} - L_{md}i'_{dr} = -L_{ds}i_{ds} - L_{md}i'_{dr} + \lambda_m \quad (7)$$

$$\lambda'_{qr} = \left(L'_{ls} + L_{mq}\right)i'_{qr} + L_{mq}i'_{qs} = L'_{qr}i'_{qr} + L_{mq}i_{qs} \quad (8)$$

$$\lambda'_{ds} = \left(L'_{lr} + L_{md}\right)i'_{dr} + L_{md}i'_{ds} = L'_{dr}i'_{dr} + L_{md}i_{ds} \quad (9)$$

Equations (6) through (9) can be merged as (10).

$$\begin{bmatrix} \lambda_{qs} \\ \lambda_{ds} \\ \lambda'_{qr} \\ \lambda'_{dr} \end{bmatrix} = \begin{bmatrix} -L_{ls} & 0 & L_{mq} & 0 \\ 0 & -L_{ls} & 0 & L_{md} \\ L'_{lr} & 0 & L'_{qr} & 0 \\ 0 & L'_{lr} & 0 & L_{dr} \end{bmatrix} \begin{bmatrix} i_{qs} \\ i_{ds} \\ i'_{qr} \\ i'_{dr} \end{bmatrix} + \begin{bmatrix} 0 \\ \lambda_m \\ 0 \\ 0 \end{bmatrix} \quad (10)$$

Equations (6) through (9) can be deduced from equations (11) through (14) if we neglect stator variables associated with the rotor and rotor variables associated with the stator.

$$\lambda_{qs} = -\left(L_{ls} + L_{mq}\right)i_{qs} = -L_{qs}i_{qs} \quad (11)$$

$$\lambda_{ds} = -\left(L_{ls} + L_{md}\right)i_{ds} = -L_{ds}i_{ds} + \lambda_m \quad (12)$$

$$\lambda'_{qr} = \left(L'_{lr} + L_{mq}\right)i'_{qr} = L'_{qr}i'_{qr} \quad (13)$$

$$\lambda'_{dr} = \left(L'_{lr} + L_{md}\right)i'_{dr} = L'_{dr}i'_{dr} \quad (14)$$

where

$$\left.\begin{aligned} L_{qs} &= L_{mq} + L_{ls} \\ L_{ds} &= L_{md} + L_{ls} \\ L'_{qr} &= L_{mq} + L'_{lr} \\ L'_{dr} &= L_{md} + L'_{lr} \end{aligned}\right\} \quad (15)$$

λ_m is the flux linkage due to permanent magnet linking the stator, ω_e is the generator electrical angular velocity in radian per seconds, i_{qs} is the stator current in the q-axis, i_{ds} is the stator current in the d-axis, L_{qs} is the stator inductance in the q-axis, L_{ds} is the rotor inductance in the d-axis, i'_{qr} is the rotor current in the q-axis, i'_{dr} is the stator current in the d-axis, L'_{qr} is the rotor inductance in the q-axis, L'_{dr} is the rotor inductance in the d-axis. L_{mq} is the stator-rotor mutual inductance in the q-axis, L_{md} is the stator-rotor mutual inductance in the d-axis, L_{ls} and L'_{lr} are the stator and the rotor leakage inductance respectively.

The flux linkage per phase between the stator and the rotor at the airgap, is deduced as:

$$\lambda_a = \sqrt{\lambda^2_{qs} + \lambda^2_{ds}} \tag{16}$$

So, by neglecting the homopolar components, and by substituting equations (11) through (14) into (1) through (4) respectively, and eliminating the flux linkage terms, the voltage equations are expressed as equations (17) through (20).

$$v_{qs} = -\omega_e L_{qs} i_{qs} + \omega_e \lambda_m - i_{qs}\left(L_{qs} + r_m\right) \tag{17}$$

$$v_{ds} = \omega_e L_{qs} i_{qs} - i_{ds}\left(L_{ds} + r_m\right) \tag{18}$$

$$v'_{qr} = \left(L'_{qr} + r_r\right) i'_{qr} \tag{19}$$

$$v'_{dr} = \left(L'_{dr} + r_r\right) i'_{dr} \tag{20}$$

The equivalent resistance, r_m , expressed in terms of the stator and core loss resistance, r_c as (21)

$$r_m = \frac{r_s \times r_c}{r_s + r_c} \tag{21}$$

The three-phase stator terminals of the IPMSG with are connected to a balanced three-phase capacitance in parallel with the load. The capacitor equations in dq reference frame are given as:

$$pv_{cqs} = q_{pm} - \omega_e v_{cqs} + \frac{i_{qs} - i_{dL}}{C} \tag{22}$$

$$pv_{cds} = \omega_e v_{cds} + \frac{i_{ds} - i_{dL}}{C} \tag{23}$$

where

$$\left.\begin{aligned} i_{cqs} &= i_{qs} + i_{qL} \\ i_{cds} &= i_{ds} + i_{dL} \end{aligned}\right\} \tag{24}$$

q_{pm} is the constant charge produced by the permanent magnet, C is the capacitance of the capacitor, v_{cqs} and v_{cds} are the q-axis capacitor voltage and the d-axis capacitor voltage respectively, i_{qL} and i_{dL} are the q-axis load current and the d-axis load current respectively.

The IPMSG is loaded with resistive and inductive loads connected in series. Treating the resistive and inductive circuit together, equation (25) and (26) are deduced for the d-q load currents.

$$pi_{qL} = \frac{v_{qL} - R_L i_{qL} - \omega_e L_L i_{dL}}{L_L} \tag{25}$$

$$pi_{dL} = \frac{v_{dL} - R_L i_{dL} + \omega_e L_L i_{qL}}{L_L} \tag{26}$$

i_{dL} is the d-axis load current

i_{qL} is the q-axis load current.

The inductive load is determined from [32] as expressed in (27):

$$L_L = \frac{R_L}{\omega_e} \times \sqrt{\left(\frac{1}{\cos\phi}\right)^2 - 1} \tag{27}$$

$\cos\phi$ is the load power factor.

$$P_{out} = \left(\frac{3}{2}\right)\omega_e \left[-\lambda_{qs} i_{ds} + \lambda_{ds} i_{qs}\right] \tag{28}$$

Equation (28) gives the relation between the electrical speed and the mechanical speed.

$$\omega_e = P_r \omega_r \tag{29}$$

where P_r is the number of pole pairs and ω_r is the mechanical speed of the rotor in radians per second. So, the output power can also be written as (30).

$$P_{out} = \left(\frac{3 P_r}{2 2}\right)\left(\omega_r \left[-\lambda_{qs} i_{ds} + \lambda_{ds} i_{qs}\right]\right) \tag{30}$$

Accordingly, the electromagnetic torque of the generator which is power divided by mechanical speed can be deduced from (30) in $d-q$ reference frame as (31).

$$T_e = \frac{P_{out}}{\omega_r} = \frac{3 P_r}{2 2}\left[\lambda_{ds} i_{qs} - \lambda_{qs} i_{ds}\right] \tag{31}$$

We know that flux is a product of inductance and current. By substituting the $d-axis$ and $q-axis$ flux linkages of equation (11) and (12) into equation (31), we have

$$T_e = \frac{3 P_r}{2 2}\left[L_{qs} - L_{ds}\right] i_{qs} i_{ds} + i_{ds} \lambda_m \tag{32}$$

Equation (32) shows that the produced electromagnetic torque is composed of two distinct mechanisms. The first term corresponds to "the reluctance torque" due to the differences of $q-axis$ and $d-axis$ reluctance (or inductance), while the second term corresponds to "the mutual reaction torque" occurring between i_{ds} and the permanent magnet. Usually, it is taken that in order to produce additive reluctance torque, i_{ds} must be negative since $L_{qs} > L_{ds}$.

The mechanical coupling equation relating to mechanical (rotational) speed in terms of developed electromagnetic torque is descried as:

$$p\omega_r = \frac{P_r}{2J_T}\left(T_e - T_L\right) \tag{33}$$

where T_L is the load torque.

J_T is the combined moment of inertia of the rotor and the driving shaft.

Equations (17) through (20) suggest the dynamic equivalent circuit of the IPMSG with rotor cage in d-q frame illustrated in Figure 2 where the capacitor, load resistance and inductance are represented, including their associated currents.

Figure 2 The d-q dynamic equivalent circuit of the three-phase rotor cage IPMSG, (a) d-axis (b) q-axis.

3.Solutions to the IPMSG equations

Saturation effects were considered in the dynamic study of the IPMSG. To account for the effects of saturation, a nonlinearity parameter has been incorporated by using polynomial fits of a machine with determined parameters expressed as a function of flux linkages which are used to adjust the inductances instead of constant inductance values. The saturation of the characteristic of the magnetizing inductance in d-q axis and the core loss resistance can be expressed mathematically in the form:

$$\begin{bmatrix} L_{qs} \\ L_{ds} \\ R_c \end{bmatrix} \cong Y_o + Y_1 \lambda_a^1 + Y_2 \lambda_a^2 + \ldots . Y_n \lambda_a^n \tag{34}$$

where $Y_o \ldots . Y_n$ are constants depending on the design of the machine.

For the studied machine, a 4th order polynomial fits of the d-q axis inductances and core loss resistance were calculated as described and given in companion paper [33], as (35) and (36) respectively. It is seen that the d-axis, the q-axis inductances and the core loss resistance are not constants but depend on the value of the magnetizing flux linkage.

$$\begin{matrix} L_{qs} \\ L_{ds} \end{matrix} = \begin{bmatrix} 3.476\lambda_a^4 - 6.734\lambda_a^3 + 2.659\lambda_a^2 - 0.410\lambda_a + 0.234 \\ 10.2\lambda_a^4 - 12.334\lambda_a^3 + 5.90\lambda_a^2 - 1.45\lambda_a + 0.183 \end{bmatrix} \tag{35}$$

$$R_c = -67.204\lambda_a^4 + 47.606\lambda_a^3 - 9039\lambda_a^2 - 93135\lambda_a + 553.42 \tag{36}$$

4.Solutions to the IPMSG dynamic equations

The load characteristics here are deduced by loading the generator on a constant load. For a given power factor loading, only the value of R_L is adjusted for a corresponding value of L_L to reach the terminal voltage. The required value of capacitor was selected as in companion paper [33]. Other relevant component reductions and optimizations were made on the simulation environment and the responses used to make design refinements. Table 1 shows the machine electrical parameters for the purpose of digital simulation. The simulation was performed using embedded MATLAB Function.

Table 1: Studied machine electrical parameters

Parameters	Values
voltage	110 volts
Stator resistance (R_s)	0.7 Ω
Rotor resistance in q-axis (R_{qr})	1:4 Ω
Rotor resistance in d-axis (R_{dr})	1:1 Ω
Number of poles	4

Frequency	50 Hz
Rotor inductance in q-axis (L_{qr})	0.0022 H
Rotor inductance in d-axis (L_{dr})	0.0024 H
Stator leakage inductance (L_{ls})	0.002 H
Unsaturated d-axis magnetizing inductance (X_{ds})	0.234 H
Unsaturated q-axis magnetizing inductance (X_{qs})	0.183 H
Capacitance of capacitor	72 µF
Rotor initials	0.0882 kg m
Power	1.250 kVA
Constant PM flux	0.8
Constant charge due to PM	0.8

5. Results and discussion

Results the magnetizing characteristic of the IPMSG

The results of the calculated saturation curve relating to the q-axis and the d-axis inductances at no-load are shown in Figure 4. It is seen that the magnetizing characteristic of the IPMSG results in a remarkable increase in the q-axis unsaturated inductance, L_{qs}. The unsaturated L_{qs} (0.234 mH) is higher than the unsaturated d-axis inductance, L_{qs} , (0.138 mH) because the magnet is in the flux path. Due to the magnetic saturation in the q-axis, L_{qs} decreases as magnetizing current, I_m , increases. On the other hand, the, L_{ds} is fairly constant as d-axis current, I_{ds} , increases due to cross-magnetizing effect of I_{ds} on the rotor magnet.

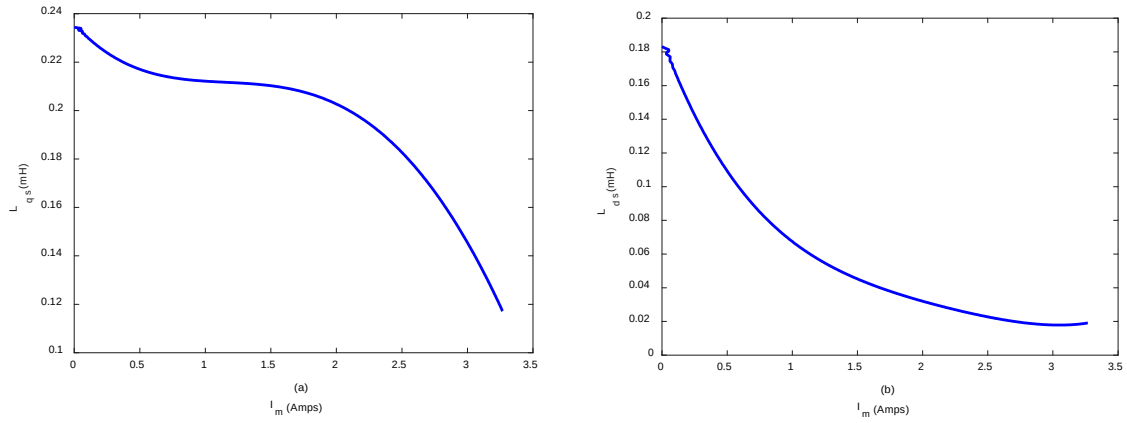

Figure 4 The d-q inductance variations of the IPMSG with magnetizing current, (a) stator-axis inductance (b)stator d-axis inductance.

Dynamic Results of the IPMSG on constant load and constant capacitor

The dynamic results of the IPMSG when the generator was made to operate at constant Resistive-Inductive load of (R=400 Ω, L=30 mH) at a unity power factor is illustrated in Figure 5 through Figure 6. The initial oscillation started at about 0.12 second for voltage build-up, and lasted to about 0.4 seconds before the voltage was stable at 140 Volts as shown in Figure 5. At that peak voltage, the electromagnetic torque was 3.3N/m. Also, in Figure 6 the phase current was 3 Amps while the load current and the capacitor current were 0.2 Amps and 2.8 Amps respectively. It is seen that much of the generator current flows to the capacitor branch and just a fraction flows to the load. This implies that all of the power will not be available to the load.

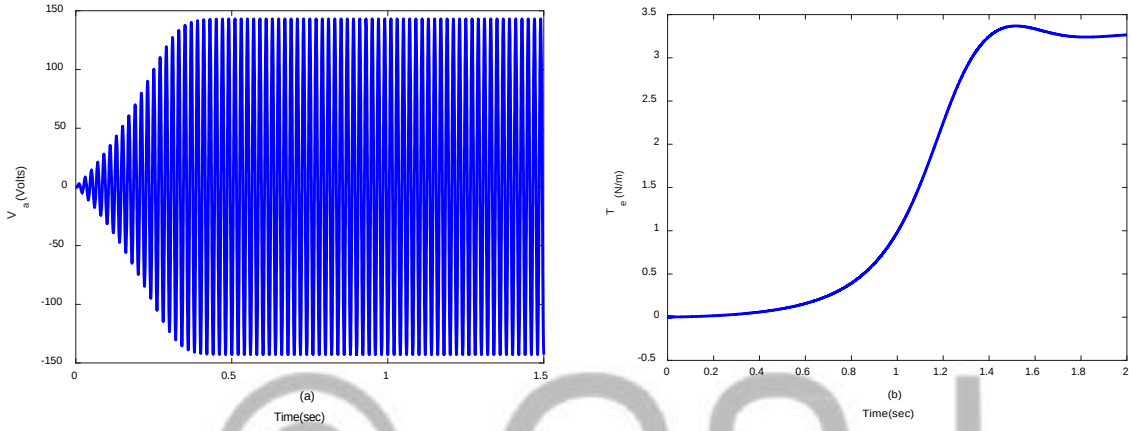

Figure 5 Dynamic response of the rotor cage IPMSG generator voltage and electromagnetic torque at constant capacitance and load, (a) stator (peak-to-peak) phase voltage (b) electromagnetic torque.

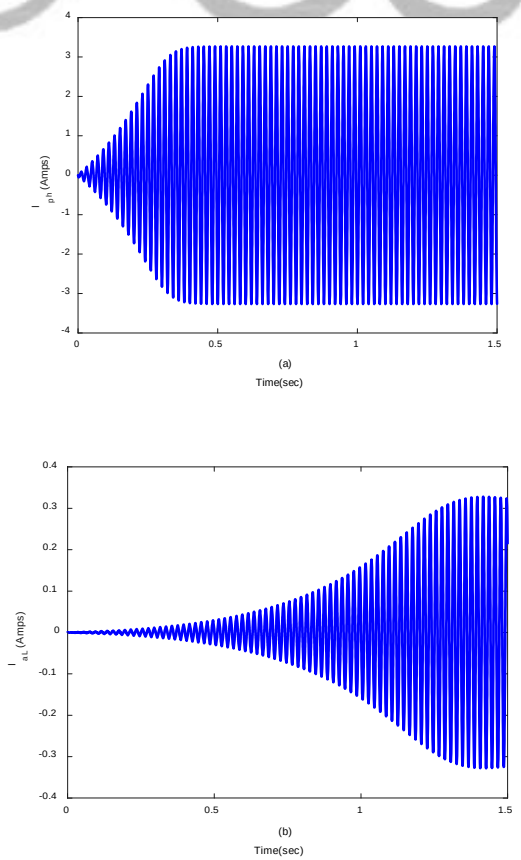

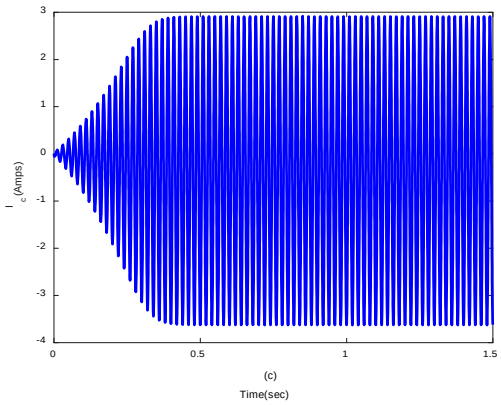

Figure 6 Dynamic response of the rotor cage IPMSG generator voltage and electromagnetic torque at constant capacitance and load, (a) stator (peak-to-peak) phase current (b) load current (c) capacitor current.

Transient Results of the IPMSG on constant load and capacitor variation

The transient results of the generator to demonstrate the effect of change in excitation capacitor is presented in Figure 7 and 9. The capacitance was made to change from 72 µF to 52 µF and then to 32 µF. The corresponding transient time of change is from 0 to 1 seconds and then 1.5 seconds. The change in the capacitance and the corresponding voltage build-up and the electromagnetic torque are is illustrated in Figure 7. In Figure 8, the stator phase current, load current and capacitor current are shown while the $d-q$ stator current are illustrated in Figure 9. The behavior of the generator with respect to the performance parameters indicates that increase in capacitor capacitance yields more voltage and electromagnetic torque. However, more current is still found in the capacitor branch than the load unit, as shown in Figure 10.

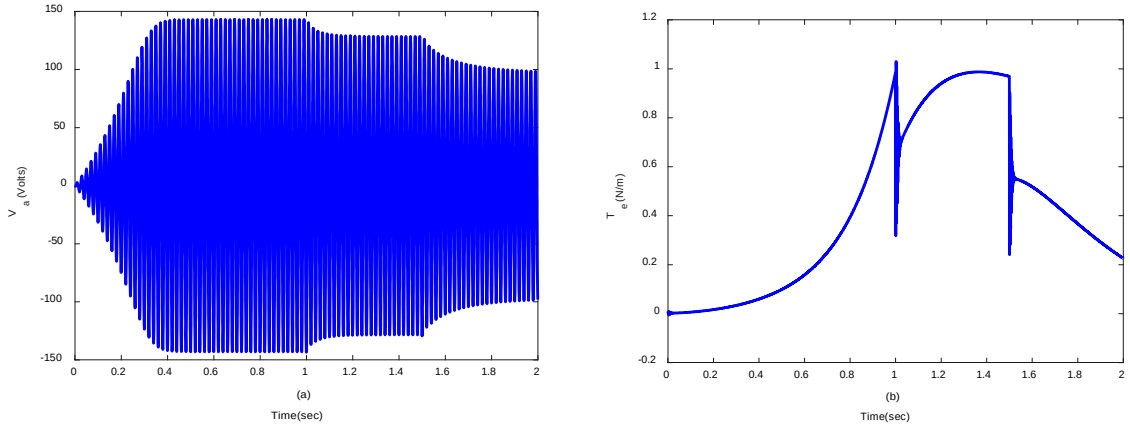

Figure 7 Transient response of the rotor cage IPMSG generator voltage and output power due to change in capacitor, (a) stator (peak-to-peak) phase voltage (b) electromagnetic torquer.

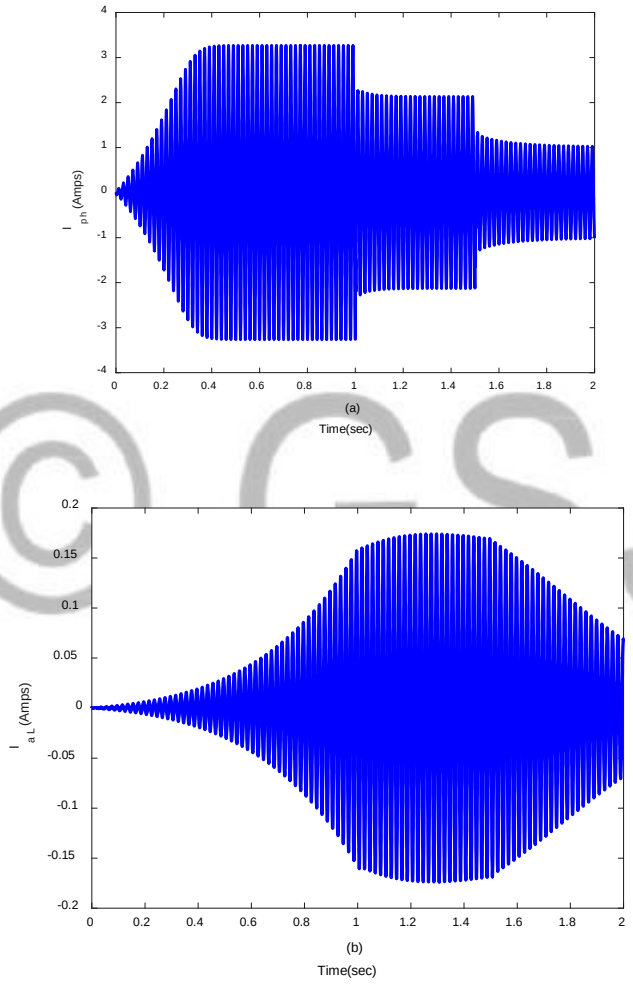
I pn (Amps)
(a)
Time(sec)
I a L (Amps)
(b)
Time(sec)

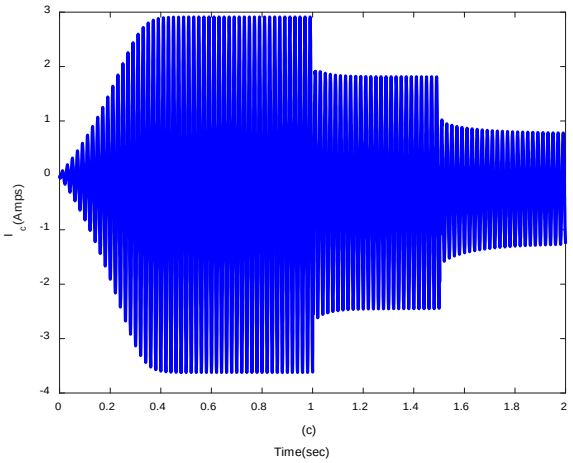

Figure 8 Transient response of the rotor cage IPMSG generator stator phase current, load current and capacitor current due to change in capacitor, (a) stator(peak-to-peak) phase current (b) load current (c) capacitor current.

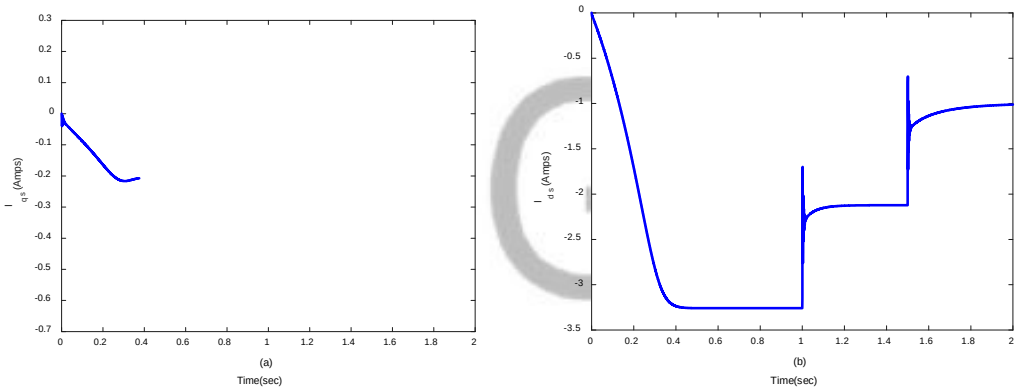

Figure 9 Transient response of the cage rotor IPMSG generator stator d-axis and q-axis current due to change in capacitor, (a) d-axis stator (peak) current (b) q-axis stator (peak) current.

3. Conclusion

This paper has presented an analysis valid to predict the dynamic characteristic of a caged rotor IPMSG with capacitor assistance. The dynamic performance analysis of the generator shows that the capability of the generator can be improved if the capacitance of the capacitor is increased. Most of the generator current flows through the capacitor branch. The addition of capacitor contributed in increasing the voltage build-up. Improving the voltage implies enhancement of the electromagnetic torque and output power. Therefore, capacitor inclusion did not only enhance the voltage, it also increased the electromagnetic torque. The obtained performance characteristics represent the basic tools required to develop a complete control system to regulate the generated voltage over a wide range of capacitor variations.

References

[1] N. R. Malik, "Analysis and control aspects of brushless induction machines with Rotating Power Electronic Converters", PhD thesis, Royal Institute of Technology, Stockholm, Sweden, November 2012.

[2] S. Ademi and M. Jovanovic, "Control of doubly fed reluctance generator for wind power application", *Elsevier* (on line), June 2015.

[3] M. Jovanovic and R. Betz R, "Power factor control using brushless doubly fed reluctance machines", in annual *meeting of IEEE Industry Applications Society*, pp. 523-530, 2000.

[4] A. S. O. Ogunjuyigbe, A. A. Jimoh, D. V. Nicolae, E. S. Obe, "Analysis of synchronous reluctance machine with magnetically coupled three-phase windings and reactive power compensation", *IET Electr. Power* Appl., vol. 4, no. 4, pp. 291– 303, 2010.

[5] L. U. Anih, "The performance characteristic of coupled round and salient pole synchronous machines", PhD thesis, University of Nigeria, March 1999.

[6] L.U. Ahih, E.S. Obe and S. E. Abonyi, "Modelling and Performance of Hybrid synchronous reluctance machine with adjustable Xd/Xq ratio", *IET power application*, August, 2014.

[7] M. A. Al-Saffar, E. Nho, T. A. Lipo, "Controlled shunt capacitor self-excited induction generator", *IEEE Trans. Energy Convers*, 1998.

[8] N. H. Malik, S. E. Hague, "Steady state analysis and performance of an isolated self-excited induction generator," *IEEE transactions on energy conversion*,1986.

[9] E. Bim , "Voltage compensation of an induction generator with long-shunt connection", *IEEE, Tran. Energy Convers*, vol. 4, no. 3, 526-530, 1989.

[10]]. S. C. Kuo and L. Wang, "Analysis of isolated self-excited induction generator", *IEEE Proceedings on Generation, Transmission and Distribution*, vol. 149, pp. 90-97, 2002.

[11] A. S. O. Ogunjuyigbe, T. R. Ayodele and, B. B. Adetrkon, "Steady state analysis of wind driven self-excited reluctance generator for isolated application", *Journal of Electric power systems research*, vol. 114, pp. 983-1004, 2017.

[12] B. J. Chalmers, "Performance of interior type permanent magnet alternator," *IEE Proc., Electr. Power Appl*, 1994, 141, no. 4, pp. 186-190.

[13] Chan, T. F., Yan, L.-T., and Lai, L. L, "Analysis and performance of a three-phase a.c. generator with inset NdFeB rotor," *Presented at Conf. on Advances in Power System Control, Operation and Management* (APSCOM-2000), Hong Kong, 2000, pp. 436-440.

[14] T. F. Chan, "Steady state analysis of self-excited synchronous reluctance generator", *IEEE Trans Energy Convers*, vol.7, no.1, pp. 223-230, March 1992.

[15] Chan, T. F., Yan, L.-T., and Lai, L. L, "Analysis and performance of a three-phase a.c. generator with inset NdFeB rotor", Presented at Conf. on Advances in Power System Control, Operation and Management (APSCOM-2000), Hong Kong, 2000, pp. 436-440.

[16] T. F. Chan, L.T. Yan, and, L. L Lai, "Performance of a three-phase a.c. generator with inset NdFeB permanent-magnet rotor", *Proc. IEEE Int. Electric Machines and Drives Conf. (IEMDC 2001)*, Cambridge, USA, pp. 652-657, June 17-20 2001.

[17] A. Rahman, A. M. Osheiba, T. S. Radwan and E. S. Abdin, "Modelling and controller design of an isolated diesel engine permanent magnet synchronous generator," *IEEE Trans. Energy Convers*., 1996, vol.11, no.2, pp. 324-330.

[18] Z. Chan, E. Spooner, W.T. Norris and A. C. Williamson, "Capacitor-assisted excitation of permanent magnet generators", *IEEE Proc. Electr. Power. Appl*. vol. 145, no.6, November 1998.

[19] N. Naoe, "Voltage compensation of permanent-magnet generator with capacitors", *Proc. 1997 Int. Conf. on Electric Machines and Drives*, Milwaukee WI, 18–21 May 1997, pp. WB2-14.1.

[20] N. Naoe, “Fundamental characteristics of voltage compensation type permanent magnet generator” EMPD95.

[21] K. J. Binns and A. Kurdali, "Permanent magnet a.c generators," *Proc. IEE*, vol. 127, no. 7, July 1979.

[22] T. F. Chan, L.T. Yan, and, L. L Lai, "Permanent-magnet synchronous generator with inset rotor for autonomous power-system applications," *IEE Proc.-Gener. Transn. Distrib.*, vol. 151, no. 5, September 2004.

[23] Fukami, Y. Matsui, T. Hayamizu, K. Shima, R. Hanaoka, and S. Takata: "Steady-state analysis of a permanent-magnet-assisted salient-pole generator," *IEEE Trans. Energy Conversion*, vol. 25, no. 2, pp. 388-393, 2010.

[24] K. Shima, N. Hirano, K. Iitomi, T. Tsuda, T. Fukami, R. Hanaoka, and S. Takata, "Analysis of reduction effect on magnetic saturation in salient pole synchronous machines by additional permanent magnets," *Proc*. ISEF2007, pp.1-4, Sep. 2007, Prague, Czech.

[25] K. J, Binns, and T. S. Low, "Performance and application of multistacked imbricated permanent-magnet generators", *IEEE Proc. B, Electr. Power Appl*., 1983, 130, no. 6, pp. 407-414.

[26] W. Wu, E. Spooner, and B. J, Chalmers, "Design of slotless torus generators with reduced voltage regulation", *IEEE Proc., Electr. Power Appl*., 1995, 142, no. 5, pp. 337-343.

[27] B. J. Chalmers, W. Wu and, E. Spooner, "An axial-flux PM generator for gearless wind energy system", *IEEE Trans. Energy Convers*., 14, no. 2, pp. 251-257,1999.

[28] E. C. Obuah and I. Briggs, "Dynamic characteristic of permanent magnet assisted synchronous reluctance generator, *International Journal of Electrical Machines & Drives*, vol.4, no. 1, pp.1-5.,2012.

[29] A. Rolan, A. Luna,,G. Vazquez, D. Aguilar and G. Azevedo, "Modeling of a variable speed wind turbine with a permanent magnet synchronous generator", *IEEE International Symposium on Industrial Electronics* (ISlE 2009), Seoul Olympic Parktel, Seoul, Korea July 5-8, 200

[30] E. Hossain, J. Hossain, N. Sakib and R. Bayindir, Modelling and simulation of permanent magnet synchronous generator wind turbine: a step to microgrid technology", *International Journal of Renewable Energy Research*, vol.7, no.1, 2017

[31] A. A. Arkadan and N. A. Demerdash, "Modelling of transients in permanent magnet synchronous generators with multiple damping circuit the natural abc frame of reference", *IEEE Trans. Energy Convers.*, 3, no. 3, pp. 722-731,1988.

[32] A. A. Arkadan and N. A. Demerdash, "Modelling of transients in permanent magnet synchronous generators with multiple damping circuit the natural abc frame of reference", *IEEE Trans. Energy Convers.*, 3, no. 3, pp. 722-731,1988.

[33] E. S. Obe and L. U. Anih. "Influence of rotor cage on the Performance of a synchronous reluctance generator," *Journal of Electric Power Components and Systems*, vol.38, pp 960-973, 2010.